Nano-Crystalline Cellulose as a Novel Tablet Excipient for Improving Solubility and Dissolution of Meloxicam

Laila H. Emara[a*], Ahmed A. El-Ashmawy [a], Nesrin F. Taha[a], Khaled A. El-Shaffei[b], El-Sayed M. Mahdey[b], Heba K. El-kholly[c]

[a]Industrial Pharmacy Laboratory, Medical and Pharmaceutical Chemistry Department, Division of Pharmaceutical Industries, National Research Centre, 33 EL Bohouthst. (former EL Tahrirst.), Dokki, Giza, Egypt. [b] Faculty of Science, Helwan University, Cairo, Egypt. [c]Advanced Materials and Nanotechnology Group, Center of Excellence for Advanced Science, National Research Centre, Giza, Egypt.

ARTICLE INFO

ABSTRACT

This study explored the effect of nano-crystalline cellulose (NCC) on Meloxicam (MX) solid dispersion (SD) prepared by co-grinding technique compared to micro-crystalline cellulose (MCC) in presence of lactose. MX-tablets were prepared by direct compression of different co-ground SDs or physical mixtures. The solubility, dissolution, SEM and DSC of different preparations were studied. Flow-through cell apparatus (FTC) was used to study the dissolution of MX from tablets at pH 7.4. Generally, the results revealed that increasing NCC loadings showed a direct increase in both the solubility and dissolution of MX. MCC did not improve either the solubility or the dissolution of MX in the physical mixture, while, co-grinding dramatically decreased the dissolution rate of MX. It was interesting to find that grinding of MX-powder alone or in a mixture with lactose highly increased MX solubility and dissolution. SEM as well as DSC were found to be very good tools, without a single exception, to describe the observed solubility and dissolution of MX in these proposed preparations. SEM-images showed the particle size reduction upon grinding or co-grinding techniques. While DSC-data proved that the crystalline structure of MX has been changed to an amorphous state.

INTRODUCTION

It is known that the rate of dissolution of a drug is a function of its intrinsic solubility and particle size. Studies with poorly soluble drugs have demonstrated that particle-size reduction to the sub-micron range can lead to an increase in dissolution rate and hence higher bioavailability (Leuner and Dressman, 2000; Patravale *et al.,* 2004; Rabinow, 2004; Kesisoglou *et al.,* 2007; Ambrus *et al.,* 2009). However, the effect of the use of nano-excipient for the formulation of poorly water soluble drugs has not yet been investigated. Cellulose has a long history in pharmaceutical industry. Despite an extended history of use in tableting, there is still continuing research into the use of new types of cellulose (viz. nanocellulose) in advanced

advanced drug-loaded systems (Lin and Dufresne, 2014). Micro-crystalline cellulose (MCC), the widely used tablet excipient, is purified, depolymerized alpha cellulose derived from plant sources. Cellulose is biodegradable, renewable, and the most abundant natural polymer in the world. It has highly ordered hierarchical structure starting from the parallel glucan chains forming nanosized fibrils, which are further organized in fibril aggregates (Hult *et al.,* 2001). The fibrils and fibril aggregates are quite often denoted cellulose nanofibers (NCC) or microfibrils (Herrick *et al.,* 1983; Turbak *et al.,* 1983; Chakraborty *et al.,* 2005; Svagan *et al.,* 2007; Quievy *et al.,* 2010). Recently, separation of cellulose nanofibers from macroscopic cellulose fibers has become the subject of much attention due to their characteristics such as high surface-to-volume ratio and outstanding mechanical properties (Kolakovic *et al.,* 2011). There is still considerable continuing research into the use of MCC and other types of cellulose in advanced drug delivery systems whereby the rate of the drug release may be controlled by microparticle inclusion,

---

* *Corresponding Author*
Laila H. Emara, Industrial Pharmacy Laboratory, Medical and Pharmaceutical Chemistry Department, Division of Pharmaceutical Industries, National Research Centre, 33 EL Bohouth st. (former EL Tahrir st.), Dokki, Giza, Egypt. Email: lhhemara@yahoo.com

excipient layering or tablet coating (Khan and Zhu, 1999; Watanabe *et al.,* 2002; El-Maradny, 2007; Gomez-Carracedo *et al.,* 2007; Podczeck *et al.,* 2008; Baumann *et al.,* 2009; Bley *et al.,* 2009; Javadzadeh *et al.,* 2009; Knight *et al.,* 2009; Kranz *et al.,* 2009; Jackson, Letchford *et al.,* 2011). Traditional method of production of MCC that includes strongly acidic conditions leads to extensive hydrolysis of amorphous fractions and formation of short rod-like MCC fibril bundles with low aspect ratio (Kolakovic, Peltonen *et al.,* 2011). Method of production of NCC that was reported for the first time by Turbak *et al* (Turbak *et al.,* 1983) required high-energy input. However, new methods using super grinder treatment or high-pressure refiner (Chakraborty *et al.,* 2005; Yano *et al.,* 2005), microfluidizer (Zimmermann *et al.,* 2004), and high-pressure homogenizer treatment (Herrick *et al.,* 1983; Dufresne *et al.,* 1997; Nakagaito and Yano, 2005) have been proposed. All these methods led to a production of gel-like water suspension with high water content, which can be further processed into powder by spray drying (Kolakovic *et al.,* 2011) or freeze drying (Emara *et al.,* 2014). NCC is at the moment a subject of continuing research. However, to the best of our knowledge, a few applications of NCC in the pharmaceutical field have been reported (Jackson *et al.,* 2011; Kolakovic *et al.,* 2011). Pharmaceutical co-crystals are emerging as a new class of solid drugs with improved physicochemical properties, which has attracted increased interests from both industrial and academic researchers. There are two different techniques for co-crystal formation via grinding. The first method is neat grinding, which is also called dry grinding, consisting of mixing the stoichiometric co-crystal components together and grinding them either manually, using a mortar and pestle, or mechanically, using a ball mill or a vibratory mill. To date many kinds of pharmaceutical co-crystals have been successfully synthesized by neat grinding (Jayasankar *et al.,* 2006; Lu and Rohani, 2009; Myz *et al.,* 2009; Qiao *et al.,* 2011). In our previous study (Emara *et al.,* 2014), NCC prepared from lignocellulosics of water sugar-cane bagasse (SCB) by freeze drying (Emara *et al.,* 2014), was used as a tablet excipient for the formulation of a water soluble drug diltiazem hydrochloride (DTZ) immediate release (IR) tablets and compared to the conventional MCC. The results of that study showed that the co-grinding of NCC with DTZ showed an initial fast and rapid increase of dissolution rate of DTZ compared to MCC (Emara *et al.,* 2014). Therefore, the aim of this study was to evaluate the usability of freeze dried NCC prepared from SCB, as a novel tablet material, in the formulation of immediate release tablets of a water insoluble drug Meloxicam (MX) by co-grinding technique. MX has been proposed in this study as a model crystalline drug because of its poor aqueous solubility (Ambrus *et al.,* 2009). MX is a non-steroidal anti-inflammatory drug (NSAID) with anti-inflammatory, analgesic and antipyretic effects. For this purpose, the NCC was compared to the commercially available MCC (Avicel PH 101) in presence of lactose as filler. The solubility, in-vitro dissolution, SEM and DSC of un-ground and ground MX powder, physical mixtures and co-ground SDs of MX with NCC, MCC and lactose were studied.

MATERIALS AND METHODS

Chemicals and reagents

MX powder was kindly donated from Delta Pharma, Egypt. Avicel PH-101 (MCC: micro-crystalline cellulose, particle size ~50 μm) was purchased from Fluka, Switzerland. Lactose monohydrate was purchased from BDH, England. Sodium hydroxide pellets and Potassium dihydrogen orthophosphate were purchased from Laboratory Rasayan, India. Distilled water was Milli RO plus 10, sourced from Millipore, USA.

Analysis of MX

A standard curve ranging from 0.2 to 40 μg/mL in phosphate buffer (pH 7.5) was constructed. A stock solution was prepared by dissolving 5 mg of MX powder in 50 mL methanol to yield a concentration of 100 μg/mL. This solution was serially diluted with pH 7.5 phosphate buffer to yield the desired concentration range. The absorbance of the prepared solutions was measured spectrophotometrically (DU–650 UV-vis spectrophotometer, Beckman, USA) at λ_{max} 363 nm against phosphate buffer of pH 7.5 as blank. The absorbance was plotted against the concentration, and the response factor was calculated. Each concentration was analyzed in triplicate, and the mean values were calculated. A linear zero-intercept relationship was established, where the slope and regression coefficient were 0.056 and 0.997, respectively. The percent recoveries ranged from 94.12% to 108.75%, and the average response factor was 14.59 ± 1.00.

Preparation of NCC

Water sugar-cane bagasse was first dried in sunlight and then cut into small pieces (1–3 cm). The cut bagasse was grinded and the fraction passing through mesh number 60 (0.251 mm sieve size) was selected for subsequent extraction of cellulose. The ground bagasse was further dried in a hot air oven (Heraeus, USA) for 16 h at 60 °C and washed by distilled water (Milli RO plus 10, Millipore, USA) at 25 °C to remove the dust and impurities on the surface, then dried. The dried bagasse was soaked in 2:1, v/v toluene/ethanol mixture for 20 h to remove wax, pigments and oils, followed by oven-drying at 55 °C for 24 h. The dewaxed bagasse was bleached with immersing in 1.4% acidified $NaClO_2$ with pH adjusted to 3.0–4.0 by CH_3COOH, at 80 °C for 2 h to dissolve lignin. Hemicellulose were leached with 1% NaOH at room temperature for 24 h and then at 60 °C for 2 h. The residue was subsequently washed with distilled water until be neutral and then air dried. Cellulose isolated from bagasse was hydrolyzed using 65 % sulfuric acid at 30 ml/g acid-to-cellulose ratio as previously reported for softwood pulp (Roman and Gray, 2005; Dong and Roman, 2007). Acid hydrolysis was stopped by diluting with 10-fold ice water. The NCC gel was washed once, centrifuged at 5000 rpm for 25 min, and then dialyzed with regenerated cellulose dialysis membranes with 12–14 kDa molecular weight cutoff (Fisherbrand, USA) against distilled water until reaching neutral pH. The suspension was sonicated (High

Intensity Ultrasonic Processor Model VC-505, Sonics & Materials, Inc., 53 Church Hill RD. Newtown, CT, U.S.A.) for 5 min in an ice bath to avoid overheating, which can cause desulfation of the sulfate groups on the cellulose (Dong, Revol *et al.,* 1998). NCC suspension was quickly frozen by pouring liquid nitrogen into the sample container and freeze-dried (Free Zone 1.0 L Bench top Freeze Dry System, Labconco, USA) overnight to remove the solvent water. The dried product was stored under vacuum (Vacuum oven, Yamato ADP-31, Japan)**.**

Preparation of co-ground SDs and their corresponding physical mixtures

Physical mixtures as well as co-ground SDs of MX powder with excipients in different ratios were prepared (Table 1). Different formulas were manually mixed in a low density polyethylene bag (Nama *et al.,* 2008; Emara *et al.,* 2012) for 5 min. For the preparation of SDs, a fixed weight (0.5g) of the physical mixture was transferred to a mortar and co-grounded for 5 min (Jayasankar *et al.,* 2006; Lu and Rohani, 2009; Myz *et al.,* 2009; Qiao *et al.,* 2011). A triplicate of each co-ground SD was prepared and evaluated.

Preparation of MX tablets (7.5 mg/Tab)

All ingredients were weighed in their specified ratios (Table 2). Tablets were prepared from different physical mixtures (F1 & F4) or co-ground SDs (F2, F3 & F5) using the flat-faced, round punches of 6 mm diameter "Single Punch Press tablet machine, Stokes-Merrill Model 511-7-A, USA" at 1.5-tons compression force.

Solubility studies

Solubility measurements were performed according to Higuchi and Connors' method. (Higuchi and Connors, 1965). In brief, an excess amount of MX in its physical mixture or co-ground SD (Table 1) was weighed into glass stoppered test tubes containing 5 mL phosphate buffer of pH 7.5. The samples were shaken at 25 °C for 48 h in temperature-controlled shaking water-bath (Lab-Line, USA) at 250 rpm. Samples were filtered through 0.45 µm membrane filter (Mellix, USA). Appropriate dilutions of the filtrates with phosphate buffer of pH 7.5 were carried out and MX was analyzed spectrophotometrically at λ_{max} 363 nm against a blank of phosphate buffer (pH 7.5). All solubility experiments were carried out in triplicate.

Tablet characteristics

PTB (311E) 3 in 1 Hardness, Diameter and Thickness Tester (PTB 311E Tablet Testing Instument, Pharma Test Apparatebau AG, Germany) was used for determination of thickness, diameter, weight, and hardness of the prepared tablets (mean of twenty tablets for each formula was calculated).

In vitro dissolution study

The dissolution rates of MX from the prepared tablets were determined, in triplicate, by employing the closed-loop setup of the flow-through cell (FTC) dissolution tester (USP Apparatus # IV, Dissotest CE-6 equipped with piston pump CY 7-50, Sotax, Basel, Switzerland) in 900 ml phosphate buffer (pH 7.5). Each tablet was placed in the 22.6 mm diameter cell (large tablet cell) in a free tablet position (Figure 1A). The powder cell of the FTC apparatus with a diameter of 12 mm was assembled as follows: One ruby bead of 5-mm diameter was positioned in the apex of the flow-through cell. Two sieves separated by a glass microfiber filter (GF/D Whatman) and the weighed amount of powder to be studied were respectively placed on the top of the sieve. The cell was closed with the prepared insert. The complete powder cell is presented in Figure 1B. Built-in filtration system (0.7 µm Whatmann GF/F and GF/D glass micro - fiber, and glass wool) was used throughout the study.

The dissolution medium was kept at 37 ± 0.5 °C and pumped at turbulent flow rate of 8 ml/min. 10 ml samples were collected at predetermined time interval for up to 90 min and were replaced by the same volume of the fresh dissolution medium. Samples were analyzed spectrophotometrically for the content of MX at λ_{max} 363 nm against phosphate buffer (pH 7.5) set as blank.
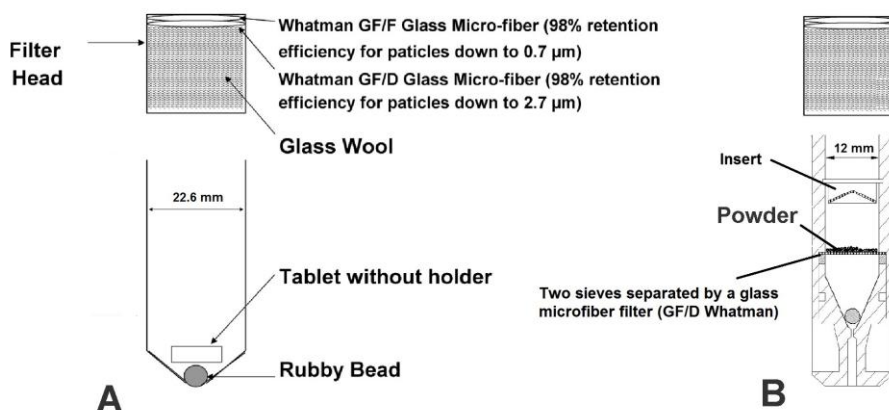

Fig. 1: Schematic diagram of the large cell (A) and the powder cell (B) of the FTC (USP Dissolution Apparatus # IV).

Table 1: Composition of different co-ground SDs, physical mixtures and their corresponding solubility data in phosphate buffer pH 7.5 at 25 °C (mean ± SD, n = 3).

Composition		Solubility (mg / 100 ml)		
MX powder	B1[a]	33.72 ± 0.48	B2[b]	55.97 ± 0.72
		Physical mixtures		**Co-ground SDs**
MX : Lactose = 1:2	B3	33.10 ± 0.53	B4	41.82 ± 0.35
MX : Lactose = 1:5	B5	32.10 ± 0.74	B6	57.47 ± 0.63
MX : Lactose = 1:10	B7	31.90 ± 0.32	B8	60.90 ± 0.47
MX : Lactose : MCC = 1:2:1	B9	33.56 ± 0.29	B10	48.39 ± 0.41
MX : Lactose : MCC = 1:2:3	B11	31.70 ± 0.55	B12	51.75 ± 0.45
MX : Lactose : MCC = 1:2:6	B13	31.14 ± 0.65	B14	51.66 ± 0.59
MX : Lactose : NCC = 1:2:0.25	B15	34.73 ± 0.48	B16	55.92 ± 0.39
MX : Lactose : NCC = 1:2:0.5	B17	31.90 ± 0.39	B18	57.11 ± 0.42
MX : Lactose : NCC = 1:2:1	B19	32.48 ± 0.59	B20	67.36 ± 0.67
MX : Lactose : NCC = 1:2:3	B21	33.10 ± 0.39	B22	64.59 ± 0.39
MX : Lactose : NCC = 1:2:6	B23	31.70 ± 0.57	B24	63.58 ± 0.71
MX : Lactose : NCC = 1:5:1	B25	32.56 ± 0.49	B26	67.38 ± 0.48

[a] Un-ground MX powder, [b] Ground MX powder.

Statistical analysis

The Dissolution profiles of different MX formulae were compared employing the fit factors $(f_1 \& f_2)$ as proposed by Moore and Flanner (Moore and Flanner, 1996), and are defined as follows [Equation (1 and 2)]:

$$f_1 = \left\{ \frac{\sum_{t=1}^{n} w_t |R_t - T_t|}{\sum_{t=1}^{n} w_t R_t} \right\} \times 100\%$$

Equation (1) and

$$f_2 = 50 \log\left\{ \left[1 + \frac{1}{n} \sum w_t (R_t - T_t)^2 \right]^{-0.5} \times 100 \right\}$$

Equation (2)

where R_t is the percentage of released drug for a reference batch at time point t, T_t is the percentage of released drug for the test batch, n is the number of time points and w_t an optional weight factor. The weight factor can be adjusted to give high or low weightings to selected time points as required. For example, if it is important to achieve a certain dissolution level by 40 min, the 40 min time point should be given a high weighting. The present study uses $w_t = 1$, meaning that each time point is weighted equally. For each batch, the calculations were made on the mean values for all the triplicates.

The factor, f_1, is the average % difference over all time points in the amount of test batch dissolved as compared to the reference batch. The f_1 value is 0 when the test and the reference profiles are identical and increases proportionally with the dissimilarity between the two profiles. Difference factor of 0-15 ensures minor difference between two products (Costa and Lobo, 2001).

The f_2 value is between 0 and 100. The value is 100 when the test and the reference profiles are identical and approaches zero as the dissimilarity increases, but because f_2 is a log function small differences in profile lead to a large drop in f_2 (Anderson *et al.*, 1998). FDA suggests that two dissolution profiles are considered similar if the similarity factor f_2 is between 50 and 100 (US-FDA, 1997).

Scanning electron microscopy (SEM)

The morphology of the pure MX, the different excipients used and selected physical mixtures and co-ground SDs of the active drug and the investigated excipients were examined by SEM (Quanta 250 FEG Model No. 1027641, Czech Republic). Each sample was sputter coated using gold sputter coating apparatus (S150A, EDWARDS, England) before SEM observation to induce electric conductivity on the surface of the samples.

Differential scanning calorimetry (DSC)

Thermal behavior of the powdered samples of MX, Lactose, MCC, NCC, selected physical mixtures and co-ground SDs containing different ratios of MX and the excipients was estimated by differential scanning calorimeter (DSC-50, Shimadzu, Japan) to investigate the state of drug in the different tested samples and to assess incompatibility if any. The samples were sealed in aluminum pans heated in an atmosphere of nitrogen and thermograms were obtained by heating at a constant heating rate of 10 °C/min in the range of 20–300 °C. A nitrogen purge (20 ml/min) was maintained throughout the run. The instrument was equipped with intra-cooler to assess thermal behavior of the sample. Alumina standard was used to calibrate the temperature and enthalpy scale of the instrument.

RESULTS AND DISCUSSION

Solubility studies

The results of solubility measurements of MX in different formulations were presented in Table 1. The reported solubility of MX at pH 7 & pH 8 were (26.6 & 155 mg/100 ml, respectively) at room temperature (23°C) (Luger *et al.*, 1996). Our study showed that the solubility of un-ground MX (B1) in phosphate buffer pH 7.5 was 33.72 ± 0.48 mg/100 ml at 25°C, While, grinding of MX (B2) pronouncedly increased the solubility of MX up to 55.97 ± 0.72 mg/100 ml. SEM images (Figures 2A&B) proved that the particle size of MX has been highly reduced and lost its crystalline structure by grinding of MX in a mortar for only 5 min.
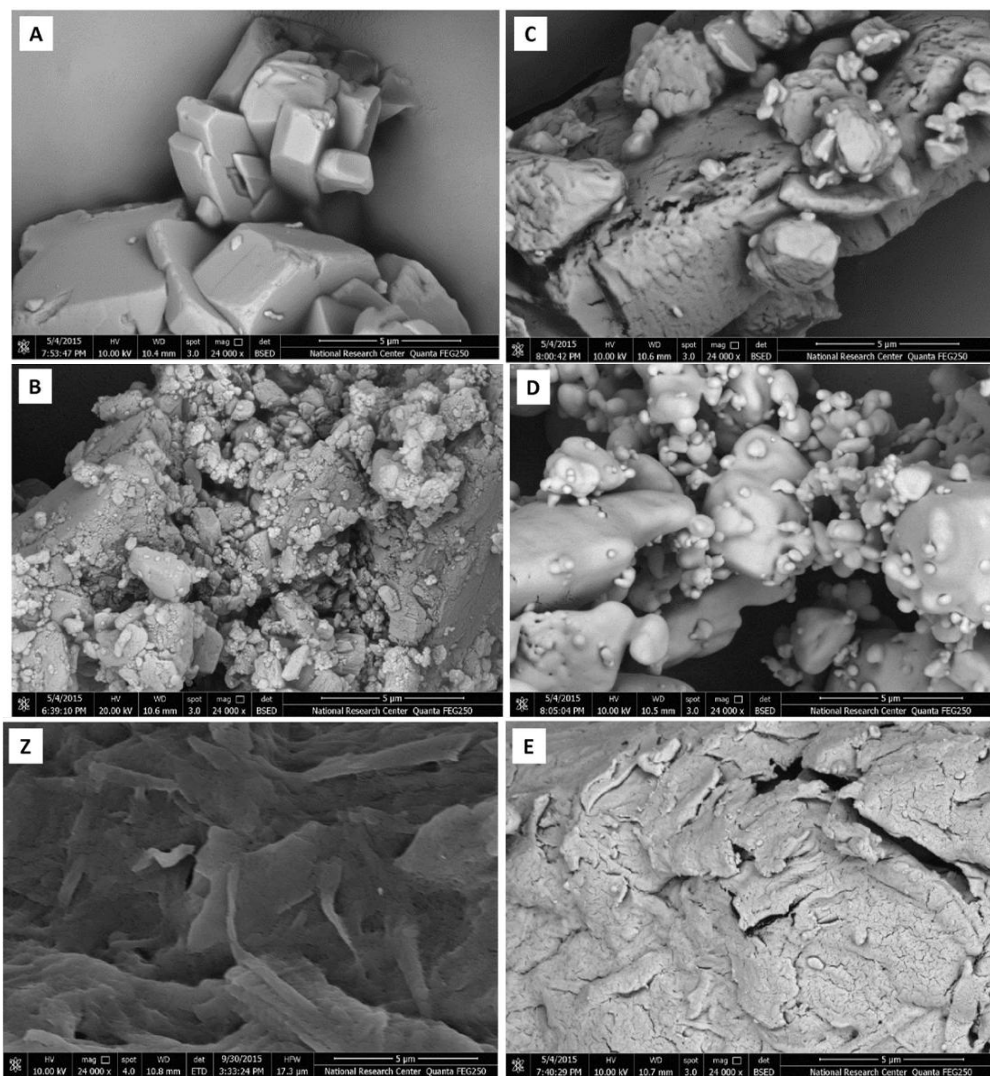
Fig. 2: SEM images of (A) = B1 (Un-ground MX); (B) = B2 (Ground MX); (C) = Un-ground Lactose; (D) = Ground Lactose; (Z) = Un-ground MCC; (E) = Ground MCC.

SEM image (Figure 2C) showed that the crystal shape of the un-ground lactose, with variable particle sizes has disappeared in the ground one (Figure 2D). Ground lactose showed the formation of very small particles with a rounded shape which was confirmed by the SEM observations (Figure 2D) and was consistent by the formation of an amorphous (or ill-crystallized) layer mainly at the surface of particles (Chikhalia *et al.,* 2006; Garnier *et al.,* 2008).

SEM image (Figure 2E) showed that the ground MCC showed a continuous plastic-like structure with the disappearance of the characteristic fiber-like structure as shown in SEM image of un-ground MCC (Figure 2Z).

All the physical mixtures of MX with lactose, NCC and MCC did not seem to increase the solubility of the drug (Table 1). On the other hand, Table 1 showed a remarkable increase in MX solubility from the co-ground SDs prepared from NCC and lactose, which ranged from 55.97 $\pm$ 0.75 mg/100 ml

(B2 ground MX) up to 67.38 $\pm$ 0.48 mg/100 ml (B26, co-ground MX/lactose/NCC). In case of co-ground SDs of MX/lactose, it was found that increasing the amount of lactose resulted in an increase in MX solubility as observed with formulae B4, B6 and B8 (Table 1). SEM images of these co-ground SDs (Figures 3F-H) showed that the crystal structure of both components in the un-ground forms (Figures 2A&C) has disappeared and gave rise to non-crystalline particles which formed a mass like structure in the ground forms as shown in Figures 2B&D. Also, this mass like structure was much more pronounced when the amount of lactose increased in the co-ground SDs (Figures 3F-H). Co-ground SDs of MX/lactose/NCC showed the highest solubilization effect with the maximum solubility of MX from B20 and B26 (Table 1). SEM images of these co-ground systems (B24, B26, Figures 3I&J) revealed that co-grinding of MX with NCC and lactose, gave rise to the dismantling of the combined mass observed with B4, B6 and B8, described in the above paragraph (Figures 3F-H), into a
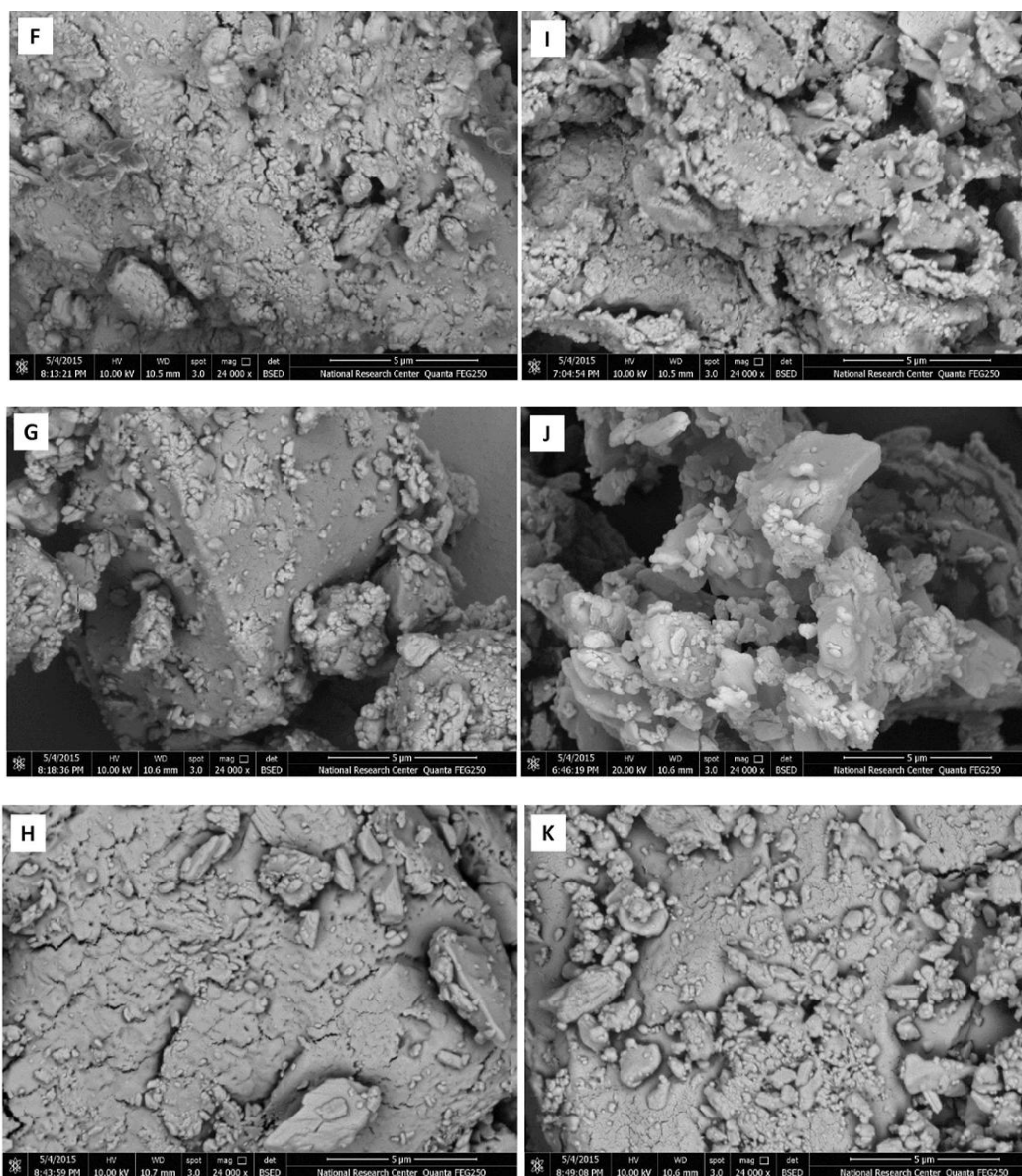
Fig. 3: SEM images of (F) = B4 (Co-ground MX : Lactose = 1 : 2); (G) = B6 (Co-ground MX : Lactose = 1 : 5); (H) = B8 (Co-ground MX : Lactose = 1 : 10); (I) = B24 (Co-ground MX : Lactose : NCC = 1 : 2 : 6); (J) = B26 (Co-ground MX : Lactose : NCC = 1 : 5 : 1); (K) = B14 (Co-ground MX : Lactose : MCC = 1 : 2 : 6).

defined small amorphous forms. It was obvious from the solubility results (Table 1) that increasing the amount of NCC in the co-ground SDs from a ratio of 1:2:1 to 1:2:6 (MX/lactose/NCC, B20 and B24, respectively) as well as increasing the amount of lactose from a ratio of 1:2:1 to 1:5:1 (MX/lactose/NCC, B20 and B26, respectively) didn't increase MX solubility. While, co-ground SDs of MX/lactose/MCC (B10, B12 and B14) gave a very slight decrease in MX solubility compared with the ground MX (B2) (Table 1). Moreover, increasing the amount of MCC did not affect the MX solubility. SEM image of co-ground SD of MX/lactose/ MCC (B14) (Figure 3K) gave an un-defined structure. It seems that MX and lactose particles were embedded within MCC particles and formed a plastic-like mass. Where, it is known that MCC is considered as a plastic material and a water insoluble

diluent (Katdare and Chaubal, 2006). Therefore, the solubility of MX was not increased. We should address here the major influence of NCC and lactose on MX solubility, which was not observed with MCC.

This means that NCC could be a very promising tablet excipient for preparing a water insoluble drug such as MX, where the inherent physical properties of MCC could be dramatically altered by nanonization techniques.

Tablet characteristics

Weight variation

The average tablet weight for F1 and F2 ranged from 44.7 − 45.2 mg, F3 and F4 (89.5 − 90.4 mg) and F5 (52.2 − 52.7 mg, cf. Table 2 for tablet composition).

Thickness and diameter

The prepared tablets showed good uniformity of thickness and diameter. The values of tablet thickness were in the range of 1.02-1.07 mm for F1, F2 and F5, 1.51-1.57 for F3 and 1.91-1.96 mm for F4. The average diameter ranged from 6.03-6.07 mm.

Hardness

Average tablet hardness ranged from 9.13 – 10.34 kp for F1 and F2, 17.9-18.3 kp for F3, 12.2-12.5 for F4 and 13.5-13.9 for F5.

Dissolution study

The disintegration time of each tablet was visually observed in the flow cell and recorded during the dissolution test. The disintegration time was variable according to the type of cellulose (MCC or NCC) incorporated in each tablet. For NCC based tablet (F3), the disintegration time was only 3 min with no visible particles after 1.5 h. While for MCC based tablet (F4), the disintegration time was $\geq$ 7 min (58 % increase in the disintegration time compared to NCC) with some particles remaining visible till the end of the 1.5 h disintegration period. The results of average tablet hardness of F3 and F4 were 18.10 and 12.35 kp, for NCC and MCC based tablets, respectively, which revealed higher compressibility of NCC compared to MCC as expected for NCC (Emara *et al.,* 2014).

Figure 4 compared the dissolution rate of un-ground and ground MX powder. It was found that a drastic increase in MX dissolution rate was achieved upon grinding the pure MX powder for 5 min. The amount of MX dissolved after 30 min (Q_{30min}) was 11% versus 43% from the un-ground and ground forms, respectively. After 60 min (Q_{60min}), 17% and 70% of MX were dissolved from the un-ground and ground drug, respectively. This means that the solubility as well as the dissolution of MX could be highly improved, simply, by grinding MX powder for 5 min due to the particle size reduction as seen in SEM images (Figures 2A&B). Where, the particle size of un-ground MX ranged from 1-7 μm (as shown in Figure 2A). While, the particle size of ground MX was highly reduced to be in a range of 0.100 – 2.5 μm, as shown in Figure 2C.

Tablets were prepared from physical mixture (F1) as well as co-ground SD (F2) of MX/lactose, in a ratio of 1:5 by direct compression (Table 2). Figure 5 revealed that F1 tablet gave higher dissolution rate in the first 30 min of the study, where, the Q_{30min} was found to be 66.49% compared to 39.27% from F1 and F2, respectively. While, Q_{60min} was 68.49% compared to 74.7 % from the above mentioned formulae, respectively. This result revealed that the tablet prepared from the physical mixture of MX/lactose resulted in a rapid onset of action and fast entry of the drug into the blood stream which might be required for the treatment of acute pain with MX.

The dissolution profiles of F1 and F2 were significantly dissimilar as depicted by the fit factors (*f1&f2)* (US-FDA, 1997) (*f1& f2*= 21 & 40", respectively). Tablets prepared by physical

mixing of MX with the water soluble diluent lactose brought the drug in close contact with this hydrophilic carrier which resulted in an increase of MX dissolution rate. This rapid dissolution rate of F1 tablet might be due to several factors such as the force applied during tablet manufacturing on the un-ground crystals of both components as in case of F1 (cf. Figure 2A & C) which might reduce the particle size of both components, solubilization effect of the carrier, improved wettability of the drug and inhibition of particle aggregation.

SEM image of co-ground SD of MX/lactose 1:5 showed different result from that of ground MX and ground lactose (Figures 2B, 2D & 3G). The co-ground MX/lactose SD resulted in a formation of large aggregates with an ill-crystallized superficial layer. In addition, we cannot neglect the mechanical force applied by direct compression of the co-ground components into tablet form, which might affect the physical nature of the drug and hence the dissolution rate.

Tablets prepared by direct compression of co-ground SDs of MX/lactose/NCC were studied in the ratios of 1:5:0 (F2), 1:5:1 (F5) and 1:5:6 (F3), respectively (Table 2).

Table 2: Composition of MX Tablets (7.5 mg / Tab).

Tablet Code	MX	Compositions (Ratio)			Form
		Lactose	MCC	NCC	
F1	1	5	----	----	Physical Mixing
F2	1	5	----	----	Co-grinding
F3	1	5	----	6	Co-grinding
F4	1	5	6	----	Physical Mixing
F5	1	5	----	1	Co-grinding

Figure 6 showed that the presence of NCC (F3 and F5) resulted in an obvious enhancement in MX dissolution rate within 30 min, compared to F2. After 30 min., 39.27%, 60.93 % and 73.84% of the amount of MX was dissolved from F2, F5 and F3, respectively. After 60 min, 74.67%, 83.57 % and 85.98 % were dissolved from F2, F5 and F3, respectively.

This means that MX dissolution rate from tablets was increased by increasing NCC loading. These results coincided with the solubility studies and proved that NCC can improve both the solubility and dissolution of MX. Comparing the dissolution profiles of F2 and F5 against F3 (set as reference) by the fit factors method. Results revealed that F3 and F5 (containing NCC) gave similar dissolution profiles (*f1&f2* = 11 and 55, respectively). While the dissolution profiles between F3 and F2 were significantly different (*f1&f2* = 27 and 35, respectively).

On the contrary to our previous study (Emara *et al.,* 2014), we have investigated the potential of addition of NCC prepared from the same batch proposed in this study (SCB) as an excipient in the preparation of tablets containing a freely soluble drug diltiazem, results showed that increasing the amounts of NCC slowed the dissolution rate of diltiazem. In this regard, we might conclude that the impact of using NCC as a tablet excipient will give different dissolution results depending on the physico-chemical properties of the drug.
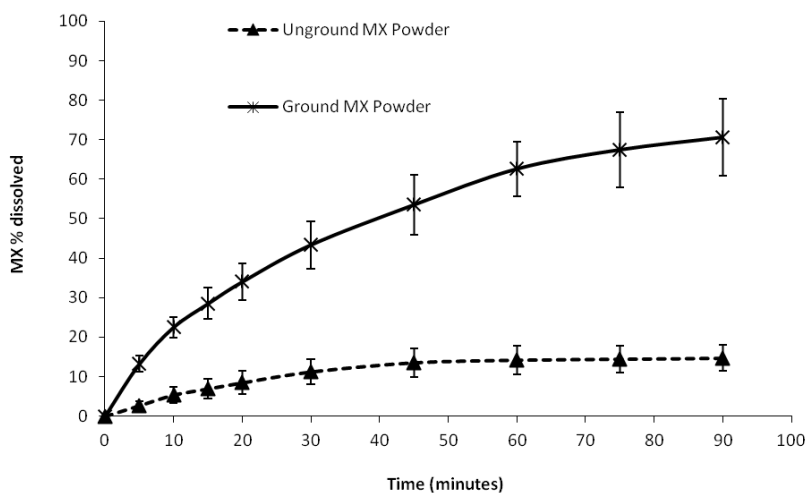
Fig. 4: Dissolution profiles of un-ground and ground MX powder (7.5 mg) using the powder cell of the FTC in phosphate buffer (pH 7.5) (*n* = 3).
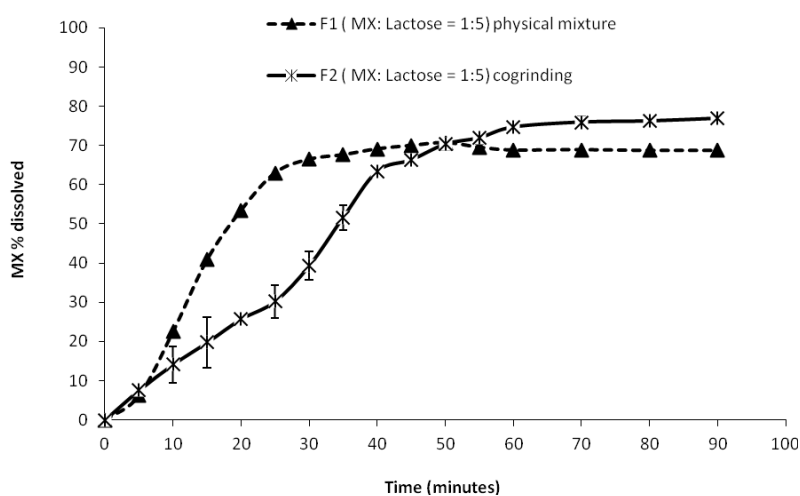

Fig. 5: Dissolution profiles of tablets containing 7.5 mg MX prepared from physical mixture of MX/lactose 1:5 (F1) and co-ground SD of MX/lactose 1:5 (F2) using the large cell of the FTC in phosphate buffer (pH 7.5) (*n* = 3).

Tablets prepared by direct compression of physical mixtures of MX/lactose and MX/lactose/MCC were studied (Table 2). Figure 7 compared the dissolution rates of physical mixtures of MX/lactose (1:5) F1 and MX/lactose/MCC (1:5:6) F4, results showed that addition of 6 parts of MCC (F4) drastically decreased the amount of MX dissolved compared to F1 (without MCC), where, after 30 min, 66.49% and 13.62 % of MX were dissolved from F1 and F4, respectively and 68.8% and 20.5% were dissolved after 60 min from the two formulae, respectively (Figure 7). Using NCC had a great effect on improving the MX solubilization as well as dissolution; in addition, presence of MCC instead of NCC dramatically decreased the dissolution rate of MX. NCC is a very promising tablet excipient in formulation of the poorly water soluble MX and the study needs further integrated and elaborated work for this important technique.

DSC

DSC was employed to investigate the crystallinity and the melting behavior of MX, lactose, NCC and MCC in the pure forms, as well as some of the ground, physical mixtures and co-ground SDs containing different ratios of MX and excipients.

The DSC thermogram of pure un-ground MX powder (Figure 8 and Table 3) exhibited a sharp endothermic peak at 260.77 °C corresponding to its melting point, with a normalized energy of -140.64 J/g (Pathak *et al.,* 2008), while the ground MX powder showed a sharper peak at almost the same melting endotherm (260.85 °C) with increased corresponding energy of -252.45 J/g, which might be an evident of the thermodynamic state variation (Glicksman, 2011).

It is known that changes in melting temperature and energy give information about, for instance, content of amorphous material (Gill *et al.,* 2010). Also, rough treatment of crystalline material, such as grinding, drying or compaction, can cause damage to the crystallinity of the material and hence increase the amorphous nature (Sebhatu *et al.,* 1994; Ford and Willson, 1999). Moreover, the amorphous forms, owing to higher molecular mobility as compared to the equivalent crystalline form, may enhance dissolution rate and this difference can then be used to estimate the degree of amorphous content in a given sample (Shah *-et al.,* 2006), which has been proved by the increase of MX solubility and dissolution by grinding.

Table 3: DSC parameters of some tested samples.

Tested samples	Code	Peak (°C)	Onset (°C)	Endset (°C)	Enthalpy (J/g)
MCC	-	105.05	36.96	147.15	-205.12
Ground MCC	-	94.40	30.41	137.30	-344.39
Ground NCC	-	83.19	27.47	133.70	-215.61
		236.27	210.12	289.00	-165.42
Lactose	-	145.14	143.69	156.30	-157.94
		217.00	211.39	222.82	-123.97
Ground Lactose	-	145.40	143.69	156.42	-174.30
		217.45	211.50	224.06	-130.09
MX	B1	260.77	258.15	269.69	-140.64
Ground MX	B2	260.85	259.46	267.71	-252.45
Co-ground SD of MX/lactose = 1:2	B4	145.99	144.13	158.22	-183.21
		217.01	211.19	224.87	-190.00
		237.72	236.94	261.03	-160.26
Co-ground SD of MX/lactose = 1:5	B6	147.43	142.57	157.46	-115.59
		217.56	210.56	225.31	-109.61
		239.14	231.33	246.93	-74.14
Co-ground SD of MX/lactose = 1:10	B8	146.77	145.00	155.91	-116.78
		216.97	210.16	223.08	-101.38
		239.94	229.83	252.42	-47.63
Co-ground SD of MX/lactose/ MCC = 1:2:6	B14	80.16	62.97	113.24	-73.56
		149.88	145.38	157.45	-30.19
		215.10	206.34	222.35	-31.68
		246.93	242.49	252.02	-31.13
Co-ground SD of MX/lactose/NCC = 1:2:6	B24	89.00	55.14	120.81	-73.90
		145.75	132.62	159.40	-15.78
		205.60	198.65	214.61	-0.95
		256.27	247.19	263.25	14.23
Co-ground SD of MX/lactose/ NCC = 1:5:1	B26	149.33	144.47	157.62	-145.98
		215.10	204.97	223.11	-113.31
		240.12	227.49	248.32	-82.23
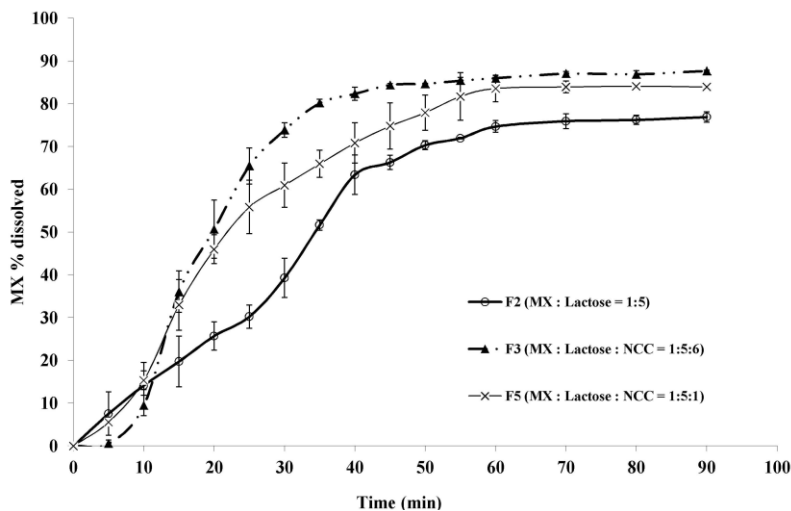
Fig. 6: Dissolution profiles of tablets containing 7.5 mg MX prepared from co-ground SD of MX/lactose 1:5 (F2); MX/lactose/ NCC 1:5:6 (F3) and MX/lactose/ NCC 1:5:1 (F5) using the large cell of the FTC in phosphate buffer (pH 7.5) (*n* = 3).

The thermograms of lactose and ground lactose showed two endothermic peaks at about 145 °C and 217 °C (Figure 8 and Table 3). However, grinding of lactose showed minor effect on its enthalpy value. The thermograms of the co-ground SDs of MX/lactose = 1:2 (B4), MX/lactose = 1:5 (B6) and MX/lactose = 1:10 (B8) (Figure 8 and Table 3) showed that the endothermic peaks of lactose were not changed. While the endothermic peak of MX was highly shifted with a reduced melting endotherm (237.72, 239.14 and 239.94 °C for B4, B6 and B8, respectively); compared to the ground MX powder. It was interesting to observe that the enthalpy was decreased for both MX and lactose as the amount of lactose increased (Table 3), This result might be an indication of the high damage to the crystallinity of both MX and lactose and hence the higher degree of amorphous content (Sebhatu *et al.,* 1994; Ford and Willson, 1999), which have been visually observed by SEM images (Figures 2A-D and 3F-H). Also, these results coincided with observed increase of MX solubility and dissolution (Table 1 and Figure 5). Moreover, the solubility of
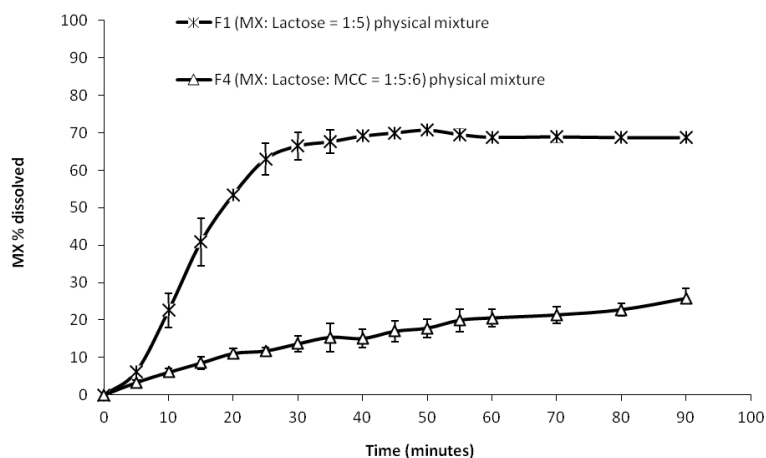
Fig. 7: Dissolution profiles of tablets containing 7.5 mg MX prepared from physical mixture of MX/lactose 1:5 (F1) and MX/lactose/ MCC 1:5:6 (F4) using the large cell of the FTC in phosphate buffer (pH 7.5) (*n* = 3).

MX was increased with increasing lactose loading as reported in Table 1. The thermograms of B6 (Co-ground SD of MX/lactose = 1:5) and B26 (Co-ground SD of MX/lactose/ NCC = 1:5:1) showed shifting of MX melting point (at 239.14 and 240.12 °C, respectively compared to ground MX powder 260.85 °C), which might be an indication of the change in MX crystallinity.
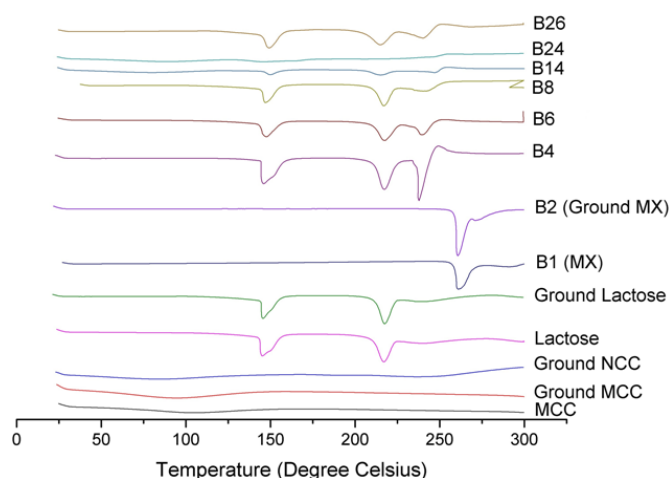

Fig. 8: DSC Thermograms of investigated samples.

A decrease of melting endotherm (enthalpy of -74.14 J/g and -82.23 J/g for B6 and B26, respectively) compared to ground MX powder (enthalpy of -252.45 J/g) was observed (Figure 8 and Table 3). This decrease in the enthalpy between ground MX (B2) compared to B6 and B26 might be due to the dilution of MX in the tested samples. On the other hand, the increase in the solubility of B26 in relation to B6 (Table 1) could be due to the different amorphous character which might be confirmed by MX peak broadness in case of B26 compared to B6 (MX peak onset – endset = 227.49 - 248.32 and 231.33 - 246.93 °C, respectively, Table 3). DSC results might be an indication of the amorphous state of MX in B6 and B26 and / or particle engineering changes which could be affecting the crystal size distribution as well as its morphology. Table 3 showed that grinding of MCC resulted in a pronounced decrease in its known

characteristic cellulose endothermic peak (Ciolacu *et al.,* 2011) from 105.05 to 94.40 °C and a high increase of enthalpy from -205.12 to -344.39 J/g for the un-ground and ground MCC, respectively).

While, the ground NCC showed appearance of a new endothermic peak at 236.27 °C with enthalpy of -165.42 J/g in addition to the characteristic cellulose endothermic peak, which has been shifted from 94.40 to 83.19 °C with enthalpy of -344.39 and -215.61 J/g, for ground MCC and ground NCC, respectively. Concerning the co-ground SDs B14 and B24 (MX/lactose/MCC =1:2:6 and MX/lactose/ NCC=1:2:6, respectively), the major change of DSC thermograms was found in the SD containing NCC (B24).

Presence of NCC in the co-ground SD showed the appearance of a new exothermic peak at 256.27 °C with enthalpy of 14.23 J/g for B24 and disappearance of the MX characteristic endothermic peak (Figure 8 and Table 3).

CONCLUSION

Based on this study, NCC might be a promising tablet excipient alternative to the widely used MCC for enhancing the solubility and dissolution of the poorly water soluble MX. Also, grinding of MX powder alone or in a mixture with lactose has greatly improved its solubility and dissolution.

DSC and SEM analysis were found to be good tools and gave decisive mirror images of both solubility and dissolution. The grinding of MX alone or with different excipients is considered a simple and environment-friendly technique which deserves further integrated studies.

ACKNOWLEDGMENT

REFERENCES

Ambrus R, Kocbek P, Kristl J, Sibanc R, Rajko R, Szabo-Revesz P. Investigation of preparation parameters to improve the dissolution of poorly water-soluble meloxicam. Int J Pharm, 2009; 381: 153-159.

Anderson N, Bauer M, Boussac N, Khan-Malek R, Munden P, Sardaro M. An evaluation of fit factors and dissolution efficiency for the comparison of in vitro dissolution profiles. J Pharm Biomed Anal, 1998; 17:811-822.

Baumann MD, Kang CE, Stanwick JC, Wang Y, Kim H, Lapitsky Y, Shoichet MS. An injectable drug delivery platform for sustained combination therapy. J Control Release, 2009; 138:205-213.

Bley O, Siepmann J, Bodmeier R. Protection of moisture-sensitive drugs with aqueous polymer coatings: Importance of coating and curing conditions. Int J Pharm, 2009; 378:59-65.

Chakraborty A, Sain M, Kortschot M. Cellulose microfibrils: A novel method of preparation using high shear refining and cryocrushing. Holzforschung, 2005; 59:102-107.

Chikhalia V, Forbes RT, Storey RA, Ticehurst M. The effect of crystal morphology and mill type on milling induced crystal disorder. Eur J Pharm Sci, 2006; 27:19-26.

Ciolacu D, Ciolacu F, Popa VI. Amorphous cellulose - structure and characterization. Cellul Chem Technol, 2011; 45:13-21.

Costa P, Lobo JMS. Modeling and comparison of dissolution profiles. Eur J Pharm Sci, 2001; 13:123-133.

Dong S, Roman M. Fluorescently labeled cellulose nanocrystals for bioimaging applications. J Am Chem Soc, 2007; 129:13810-+.

Dong XM, Revol J-f, Gray DG. Effect of microcrystallite preparation conditions on the formation of colloid crystals of cellulose. Cellulose, 1998; 5:19-32.

Dufresne A, Cavaille JY, Vignon MR. Mechanical behavior of sheets prepared from sugar beet cellulose microfibrils. J Appl Polym Sci, 1997; 64:1185-1194.

El-Maradny HA. Modulation of a pulsatile release drug delivery system using different swellable/rupturable materials. Drug Deliv, 2007; 14:539-546.

Emara L, El-Ashmawy A, Taha N, El-Shaffei K, Mahdey S, El-Kholly H. (2014). *Freeze-dried nanocrystalline cellulose derived from water sugar-cane bagasse as a novel tablet excipient.* Paper presented at the The 41st Annual Meeting & Exposition of the Controlled Release Society, Chicago, Illinois, USA; 2014: July 13 – 16.

Emara LH, Abdou AR, El-Ashmawy AA, Badr RM, Mursi NM. In vitro evaluation of floating matrix tablets of amoxicillin and metronidazole for the eradication of helicobacter pylori. Int J Pharm Pharm Sci, 2012; 4:671-681.

Ford JL, Willson R. (1999). Thermal analysis and calorimetry of pharmaceuticals. In RB Kemp (Ed.), *Handbook of thermal analysis and calorimetry* (Vol. 4: From Macromolecules to Man, pp. 923-1016): Elsevier.

Garnier S, Petit S, Mallet F, Petit MN, Lemarchand D, Coste S, Lefebvre J, Coquerel G. Influence of ageing, grinding and preheating on the thermal behaviour of alpha-lactose monohydrate. Int J Pharm, 2008; 361:131-140.

Gill P, Moghadam TT, Ranjbar B. Differential scanning calorimetry techniques: Applications in biology and nanoscience. J Biomol Tech, 2010; 21:167-193.

Glicksman ME. (2011). Thermodynamics of crystal-melt phase change *Principles of solidification, an introduction to modern casting and crystal growth concepts* (pp. 27-51): Springer.

Gomez-Carracedo A, Souto C, Martinez-Pacheco R, Concheiro A, Gomez-Amoza JL. Microstructural and drug release properties of oven-dried and of slowly or fast frozen freeze-dried mcc-carbopol (r) pellets. Eur J Pharmaceut Biopharm, 2007; 67:236-245.

Herrick FW, Casebier RL, Hamilton JK, Sandberg KR. Microfibrillated cellulose: Morphology and accessibility. J Appl Polym Sci, 1983; 37:797-813.

Higuchi T, Connors K. 1965. Phase-solubility techniques *Advances in analytical chemistry and instrumentation* (pp. 117-212): Jonh Wiley & Sons, INC.

Hult EL, Larsson PT, Iversen T. Cellulose fibril aggregation - an inherent property of kraft pulps. Polymer, 2001; 42:3309-3314.

Jackson JK, Letchford K, Wasserman BZ, Ye L, Hamad WY, Burt HM. The use of nanocrystalline cellulose for the binding and controlled release of drugs. Int J Nanomedicine, 2011; 6:321-330.

Javadzadeh Y, Shariati H, Movahhed-Danesh E, Nokhodchi A. Effect of some commercial grades of microcrystalline cellulose on flowability, compressibility, and dissolution profile of piroxicam liquisolid compacts. Drug Dev Ind Pharm, 2009; 35:243-251.

Jayasankar A, Somwangthanaroj A, Shao ZJ, Rodríguez-Hornedo N. Cocrystal formation during cogrinding and storage is mediated by amorphous phase. Pharm Res, 2006; 23:2381-2392.

Katdare A, Chaubal M. (2006). *Excipient development for pharmaceutical, biotechnology, and drug delivery systems*: CRC Press.

Kesisoglou F, Panmai S, Wu Y. Nanosizing--oral formulation development and biopharmaceutical evaluation. Adv Drug Deliv Rev, 2007; 59:631-644.

Khan GM, Zhu JB. Studies on drug release kinetics from ibuprofen-carbomer hydrophilic matrix tablets: Influence of co-excipients on release rate of the drug. J Control Release, 1999; 57:197-203.

Knight PE, Podczeck F, Newton JM. The rheological properties of modified microcrystal line cellulose containing high levels of model drugs. J Pharm Sci, 2009; 98:2160-2169.

Kolakovic R, Peltonen L, Laaksonen T, Putkisto K, Laukkanen A, Hirvonen J. Spray-dried cellulose nanofibers as novel tablet excipient. AAPS PharmSciTech, 2011; 12:1366-1373.

Kranz H, Juergens K, Pinier M, Siepmann J. Drug release from mcc- and carrageenan-based pellets: Experiment and theory. Eur J Pharmaceut Biopharm, 2009; 73:302-309.

Leuner C, Dressman J. Improving drug solubility for oral delivery using solid dispersions. Eur J Pharmaceut Biopharm, 2000;50: 47-60.

Lin N, Dufresne A. Nanocellulose in biomedicine: Current status and future prospect. Eur Polym J, 2014; 59:302-325.

Lu J, Rohani S. Preparation and characterization of theophylline-nicotinamide cocrystal. Org Process Res Dev, 2009; 13:1269-1275.

Luger P, Daneck K, Engel W, Trummlitz G, Wagner K. Structure and physicochemical properties of meloxicam, a new nsaid. Eur J Pharm Sci, 1996; 4:175-187.

Moore JW, Flanner HH. Mathematical comparison of dissolution profiles. Pharm Tech, 1996; 20:64-74.

Myz SA, Shakhtshneider TP, Fucke K, Fedotov AP, Boldyreva EV, Boldyrev VV, Kuleshova NI. Synthesis of co-crystals of meloxicam with carboxylic acids by grinding. Mendeleev Commun, 2009;19:272-274.

Nakagaito AN, Yano H. Novel high-strength biocomposites based on microfibrillated cellulose having nano-order-unit web-like network structure. Appl Phys A Mater Sci, 2005; 80:155-159.

Nama M, Gonugunta CS, Reddy Veerareddy P. Formulation and evaluation of gastroretentive dosage forms of clarithromycin. AAPS PharmSciTech, 2008; 9:231-237.

Pathak D, Dahiya S, Pathak K. Solid dispersion of meloxicam: Factorially designed dosage form for geriatric population. Act. Pharmaceut., 2008; 58:99-110.

Patravale VB, Date AA, Kulkarni RM. Nanosuspensions: A promising drug delivery strategy. J Pharm Pharmacol, 2004; 56:827-840.

Podczeck F, Knight PE, Newton JM. The evaluation of modified microcrystalline cellulose for the preparation of pellets with high drug loading by extrusion/spheronization. Int J Pharm, 2008; 350:145-154.

Qiao N, Li M, Schlindwein W, Malek N, Davies A, Trappitt G. Pharmaceutical cocrystals: An overview. Int J Pharm, 2011; 419:1-11.

Quievy N, Jacquet N, Sclavons M, Deroanne C, Paquot M, Devaux J. Influence of homogenization and drying on the thermal stability of microfibrillated cellulose. Polym Degrad Stab, 2010; 95:306-314.

Rabinow BE. Nanosuspensions in drug delivery. Nat Rev Drug Discov, 2004; 3:785-796.

Roman M, Gray DG. Parabolic focal conics in self-assembled solid films of cellulose nanocrystals. Langmuir, 2005; 21:5555-5561.

Sebhatu T, Angberg M, Ahlneck C. Assessment of the degree of disorder in crystalline solids by isothermal microcalorimetry. Int J Pharm, 1994; 104:135-144.

Shah B, Kakumanu VK, Bansal AK. Analytical techniques for quantification of amorphous/crystalline phases in pharmaceutical solids. J Pharm Sci, 2006; 95:1641-1665.

Svagan AJ, Samir MASA, Berglund LA. Biomimetic polysaccharide nanocomposites of high cellulose content and high toughness. Biomacromol, 2007; 8:2556-2563.

Turbak AF, Snyder FW, Sandberg KR. Microfibrillated cellulose, a new cellulose product: Properties, uses, and commercial potential. J Appl Polym Sci, 1983; 37:815-827.

US-FDA. Guidance for industry: Dissolution testing of immediate release solid oral dosage forms. Food and Drug Administration, Center for Drug Evaluation and Research (CDER), Rockville, MD, USA, 1997.

Watanabe Y, Mukai B, Kawamura K, Ishikawa T, Namiki M, Utoguchi N, Fujii M. Preparation and evaluation of press-coated aminophylline tablet using crystalline cellulose and polyethylene glycol in the outer shell for timed-release dosage forms. YAKUGAKU ZASSHI, 2002; 122:157-162.

Yano H, Sugiyama J, Nakagaito AN, Nogi M, Matsuura T, Hikita M, Handa K. Optically transparent composites reinforced with networks of bacterial nanofibers. Adv Mater, 2005; 17:153-+.

Zimmermann T, Pohler E, Geiger T. Cellulose fibrils for polymer reinforcement. Adv Eng Mater, 2004; 6:754-761.